Electronic Supplementary Material (ESI) for RSC Advances.
This journal is © The Royal Society of Chemistry 2014

Journal Name

Dynamic Article Links ►

Cite this: DOI: 10.1039/c0xx00000x

www.rsc.org/xxxxxx

ARTICLE TYPE

The dynamic process of radioactive iodine removal by ionic liquid 1-butyl-3-mehtyl-imidazolium acetate: discriminating and quantifying halogen bonds versus induced force

Yu Chen, Chuanyu Yan, Wancheng Zhao, Zhenghui Liu, Tiancheng Mu*

**Department of Chemistry, Renmin University of China, Beijing 100872, P. R. China*

Abstract

With the increasing demand of nuclear energy and Fukushima Daiichi nuclear disaster in 2011, the removal of radioactive and hazardous iodine has attracted more and more attention. Here, we investigate the dynamic process of radioactive iodine sorption in a representative acetate-based ionic liquids (AcILs), 1-butyl-3-methyl-imidazolium acetate [BMIM][Ac], via in situ UV-vis spectroscopy in combination with two-dimensional correlation technique. More importantly, the halogen bonds (including interior and exterior types) and induced force (only owning an exterior form) resulting in iodine sorption in [BMIM][Ac] at some specific time points are discriminated and quantified. Results show that the iodine sorption in [BMIM][Ac] can be divided into three zones. In the first 140 min, only halogen bonds occur (Zone 1). From 140 to 240 min, (exterior) halogen bonds and induced force occur simultaneously (Zone 2). After 240 min, only induced force occurs (Zone 3). Specifically, Zone 1 consists of two subzones, i.e., Zone 1a (before 90 min) and Zone 1b (90 -140 min), corresponding to interior and exterior halogen bonds, respectively. Zone 2 is constituted of three subzones, i.e., Zone 2a (140 -180 min), Zone 2b (180 - 200 min), and Zone 2c (200 - 240 min), with (exterior) halogen bonds taking up the most part, about one half, and small part of the total iodine sorption, respectively. The proportion of halogen bonds and induced force resulting in iodine sorption by [BMIM][Ac] can be derived approximately as 100% and 0% within 140 min, 96% and 4% within 240 min, 91% and 9% within 570 min, respectively. Furthermore, the proportion of interior and exterior halogen bonds resulting in iodine sorption by [BMIM][Ac] could be derived approximately as 85% and 15% within 140 min, 80% and 20% within 240 min, 80% and 20% within 570 min, respectively. These processes and quantifications can provide insight into the radioactive iodine removal by ILs in addition to [BMIM][Ac] here we investigated, and may motivate further experimental or theoretical studies on the application of halogen bonds on removal of iodine by designing new types of ILs.

1. Introduction

The utilization of nuclear energy is increasing in order to meet the energy requirements, during which nuclear waste would be released. More importantly, a large quantity of nuclear waste will be produced if nuclear accident takes place, such as Fukushima Daiichi nuclear disaster in 2011 and Chernobyl nuclear accident in 1986.[1-2] Another source of nuclear waste is from the manufacture of nuclear weapon. The above three sources of nuclear waste will definitely do harm to human health. One of the most common nuclear wastes is isotopes iodine (e.g., $^{125/129/131}$I), which is generated as the byproducts after the fission of uranium and plutonium. Particularly, ^{129}I owns a very long half-life as long as 15.7 million years, in need of a reliable entrapment and storage. ^{131}I direct affects human metabolic processes and triggers thyroid cancer in spite of its short-lived term as short as 8 days.[3-4]

Many kinds of adsorbents have been proposed for iodine capture. Silver-based zeolites, one of the inorganic solid adsorbents, are suggested to the current substance to entrap iodine with favorable capacity and removal efficiency.[5] Nevertheless, the relative low porosity and adverse environment impact limit its practical application in spite of abundant nuclear waste. The metal-organic framework (MOF) materials are then proposed to uptake iodine with enhanced capacity due to higher surface areas, and can trap iodine through pressure-induced amorphization.[6-9] Unfortunately, water-instability property of MOF may hinder a lot its practical application in the moist air. Other materials, such as molecular organic solids,[10] metalloporphyrin-based conjugated microporous polymer,[11] activated carbon,[12] cyclodextrins,[13] Ag_2O grafted titanate nanolamina,[14] silver aluminophosphate glasses[15] have also been suggested for iodine capture. However, these materials still possess the drawback of low iodine-removing capacity. Therefore, it is interesting to develop novel materials to reliably and efficiently store iodine.

We have proved that ionic liquids (ILs) could hold iodine tightly.[16] ILs are the liquid salts around the room temperature,

usually consisting of an organic cation and an organic/inorganic anion. The favorable features of ILs include the low vapor pressure, wide liquid-ranging temperature, and high thermal stability. They have attracted particularly much attention in many fields, such as sour gases capture,[17-18] chemical synthesis and catalysis,[19-20] biomass utilization,[21-22] and analytical medium[23]. Among all the types of ILs, acetate-based ionic liquids (AcILs) emerged as a unique class of liquid salts with organic cation and acetate anion that show exceptional solvation capacity in both biomass utilization[22] and carbon dioxide capture[24-25]. Also, AcILs own the favorable features of low viscosity, low melting point, easy synthesis, low cost, and high biodegradation. Like the common traits of ILs, AcILs are also highly tunable and relatively green. We have found that, one of common AcILs, 1-butyl-3-methlyl-imidazolium acetate [BMIM][Ac], showed a much higher efficiency on iodine capture than the above refereed materials, (e.g., MOF) mainly via halogen bonds.[16]

Halogen bonds, a counterpart of hydrogen bonds, have been focused on in the last two decades in many fields.[26-29] The general expression of halogens bonds is D···X-Y, where X is the electrophilic halogen atom as halogen bonds donor (e.g., F, Cl, Br, I); D is the electronegative group as the halogen bonds acceptor (O, N, pi, F, Cl, Br, I); and Y is any of other atom tethered to halogen atom X (e.g., C, F, Cl, Br, I).[30-35] Simply, halogen bonds are the intermolecular electrostatic force when a covalently-bonded halogen encounters an electronegative species.[36] The recognition of halogen bonds started in 19th century.[37] Subsequently, the solutions and solid states were studied for a better understanding of the dihalogens/electron donor association.[38-43] The broad name of "halogen bonds" in halogenated electrophiles only occurred a decade ago.[26] Since then, the halogen bonds have been widely studied in many areas, such as crystal engineering,[26] biologic molecules,[44] supramolecular materials designs,[45-47] organ ocatalysis or reactivity control[48-49] self-assembly process,[50] and rational drug design.[51-54] More interestingly, halogen bonds could also control the iodine sorption in the ILs as reported by our group.[16]

It is concluded in our previous report that [BMIM][Ac] absorbs iodine mainly via halogen bonds and little via induced force.[16] However, how is the dynamic process of iodine sorption in [BMIM][Ac]? Could we obtain the proportion of halogen bonds and induced force contributing to the iodine sorption? Furthermore, since the halogen bonds resulting in iodine sorption are induced to stay in the ILs interior, are there any possibilities for iodine to be absorbed on the ILs exterior, and what is the quantification? Understanding the microscopic sorption process and the halogen bonds ratio will help a lot to design and synthesize new ILs with higher efficiency and faster rate for radioactive iodine entrapment. We will discuss the above questions below.

Therefore, we select a representative AcIL [BMIM][Ac] (Scheme 1) to investigate the dynamic process of iodine (Scheme 1) sorption and its corresponding halogen bonds quantification because [BMIM][Ac] owns the favorable properties as discussed above. Furthermore, the ILs with higher iodine sorption capacity than [BMIM][Ac] (e.g., [BMIM][Cl], [BMIM][Br], [BMIM][I], [BMIM][TFO]) contain halogen atoms,[16] which might pose again adverse effect on the environment. Still, some of these ILs (e.g., [BMIM][Cl], [BMIM][Br], [BMIM][I]) show a solid state at the room temperature, which might hinder its application when related to the spray technology, in spite of their higher efficiency via stronger halogen bonds than [BMIM][Ac].[16] The remaining ILs (e.g., [BMIM][Tf_2N], [BMIM][PF_6], [BMIM][BF_4], [BMIM][ClO_4], [BMIM][NO_3]) absorb iodine mainly via induced force due to a less favorable halogen-bonding accepting ability of these anions than the acetate anion in [BMIM][Ac].[16] It thus will be more appropriate to select [BMIM][Ac] as a model IL to investigate the dynamic iodine sorption process and to quantify the proportion of halogen bonds and induced force. In this sense, although halogen bonds are the main contributor of iodine sorption, induced force might also play a role to some extent.

Here, we select two-dimensional correlation (2D-COS) ultraviolet visible (UV-vis) spectroscopy, i.e., 2D-COS UV, as the tool to detect this dynamic process of iodine sorption in [BMIM][Ac]. Generalized two-dimensional correlation spectroscopy (G-2D-COS) is the first technique to compare the relationship of two spectra intensity along the perturbation variable (e.g., time, temperature, concentration, PH) and to decode the subtle information from those overlapped original spectra.[55-56] Later, auto-correlation moving-windowing two-dimensional correlation spectroscopy (auto-MW2D-COS) is proposed by replacing one of two spectral variables (wavenumber and wavelength) in G-2D-COS perturbation variable with perturbation variable.[57] Recently, a more advanced technique of perturbation-correlation moving-window two-dimensional correlation spectroscopy (PCMW2D-COS) has been developed for a better discrimination of critical transition, band shift, and the complicated intensity variation along the perturbation variable.[58] Both of G-2D-COS and PCMW2D-COS include the synchronous (s-G-2D-COS and s-PCMW2D-COS) and synchronous (as-G-2D-COS and as-PCMW2D-COS) mode. Actually, the 2D-COS technique has been successfully applied to investigate the intermolecular ILs/solvent systems by Lendl,[59] Yu,[60-61] Li,[62] Wu,[63-65] and Wang,[66] and so on. Recently, we also have used 2D-COS technique to investigate the ILs/water dynamic interaction.[67] Meanwhile, UV-vis spectroscopy is probably one of the most convenient and efficient tools to detect halogen bonds.[7, 16, 36] Thus, the combination of 2D-COS and UV-vis (i.e., 2D-COS UV) can be considered as a reliable method to analyze the dynamic process of iodine sorption in [BMIM][Ac].

2. Experimental section

2.1. Materials.

[BMIM][Ac] (≥ 99%) was purchased from Lanzhou Greenchem ILs, LICP, CAS (Lanzhou, China). [BMIM][Ac] sample was loaded in a vial, which was placed in a vacuum oven at 60 ℃ for 80 h for drying before use. For a better drying efficiency, some P_2O_5 was loaded onto another vial and then put in the vacuum oven. The water content in [BMIM][Ac] was less than 790 ppm measured by Karl Fisher titration. Halogen ion was undetectable by $AgNO_3$ precipitation. NMR spectra and IR spectra before and after the drying indicated that thermal decomposition of [BMIM][Ac] during the drying process was negligible.

2.2. UV-vis spectra measurement.

0.2429 g of IL sample was loaded into the cuvette (with an

This journal is © The Royal Society of Chemistry [year]

optical length of 1 cm). Then, the sample in the cuvette was evenly distributed by ultrasonic oscillation for about 10 min. Subsequently, 1.7195 g of iodine cyclohexane solution (0.384 g/L) was added onto the [BMIM][Ac] phase at room temperature (ca. 20 °C) without stirring, followed by the seal of cuvette by a self-contained cap in order to avoid evaporation of iodine and the water uptake from the moisture air due to the high hygroscopicity of ILs.[68-69] Then, UV-vis spectroscopy (Carry 5.0, Varian) was measured to characterize the supernatant (i.e., upper phase containing iodine cyclohexane solution) and determine the iodine concentration as a function of time from 0 min to 570 min with the increment of 5 min within the wavelength range from 280 nm to 700 nm. We used the same solvent, that is, pure cyclohexane as a blank.

2.3. Difference UV-vis spectra and peak area calculation.

The difference UV-vis spectra were derived by the original UV-vis spectra as described in the above section. Specifically, we chose the starting spectra as the reference spectrum, subtracting which from the each dynamic UV-vis spectra could obtain the difference UV-vis spectra. The difference UV-vis spectra could be used to demonstrate a more obvious change in intensity. The peak area of UV-vis was calculated by the Origin Professional 9.0 by the form of absolute value.

2.4 Color change experiment.

The color change was mainly referred to the supernatant iodine solution with the cyclohexane as the solvent. The picture was taken by the commercial camera every 1 h for 10 h. Note that the contents of supernatant (ca. 0.2644 g) and subnatant (ca.1.9358 g) were slightly different from that in the cuvette aimed for UV-vis measurement. Also, here we loaded the two-phase system in a glass vial (ca. 5 mL) sealed with its self-contained cap rather than cuvette. The upper phase is the iodine cyclohexane solution, showing a violet color. The lower phase is pure [BMIM][Ac], showing a yellow color. The seemingly yellow color in the top surface in the glass bottle is not a phase but only a light reflection or refraction caused in the experimental condition. The picture is taken separately for each one by using a same white paper as the substrate, and then combined together.

2.5. ATR-IR spectra measurement.

FT-IR spectrometer (Prestige-21, Shimadzu, Japan, DTGS detector) was applied by using the attenuated total reflection (ATR-IR, with a ZnSe ATR-8200H cell, 584 mm^2 surfaces, 45° incident angles) as the accessory. Before the experiment, [BMIM][Ac] was placed on the cell without covering the seal of ATR cell and the lid of FT-IR to let a direct exposure to moisture air. Once the samples were loaded on the ATR cell, they were scanned every 5 min till 570 min, when the change of intensity and positions of all peaks was negligible after 570 min. During this process the samples on ATR cell kept static and no stirring or mixing behavior was conducted. The parameters set for each sample in ATR-IR was 40 scans, 4 cm^{-1} resolutions, and 4200 cm^{-1} wavenumber spans (ranging from 4600 cm^{-1} to 400 cm^{-1}).

2.6. G-2D-COS, auto-MW2D-COS and PCMW2D-COS.

All the two-dimensional correlation spectroscopy 2D-COS (including s-G-2D-COS, as-G-2D-COS, auto-MW2D-COS, s-PCMW2D-COS, as-PCMW2D-COS) were obtained from the original data by using the mature software (i.e., 2D *shige*, http://sci-tech.ksc.kwansei.ac.jp/~ozaki/2D-shige.htm). 2D shige was wide used in academic study, including the intra- or inter-molecular interactions related to neat ILs and their mixtures,[58, 63-64, 66] and could be uploaded form the website above suggested by Shige Morita. We set the parameter of window size ($2m + 1$) as 11 for all the data process of 2D-COS. Then, we plotted planar and stereoscopic figures with these data derived from 2D *shige*.

3. Results and discussion

The overview of schemes and figures is stated before the discussion for a better overlooking of the panoramic view of this paper. Fig. 1 and 2 are the normal and difference UV-vis spectroscopy of I_2 (i.e., in the state of cyclohexane solution in the upper phase) sorption in ionic liquid (IL, in the lower phase) [BMIM][Ac] as a function of time from 0 to 570 min, respectively. The corresponding peak area with time is described in Fig. 3 and 4, the latter of which presents a slice spectrum at 660 nm. Then, we obtain the corresponding s-G-2D-COS (Fig. 5) and s-G-2D-COS (Fig. 6) spectroscopy via the 2D shige software with the UV-vis data. Furthermore, the auto-MW2D-COS (Fig. 7), s-PCMW2D-COS (Fig. 8), and as-PCMW2D-COS (Fig. 9 and 10), are derived for a better understanding of the dynamic process of iodine sorption in [BMIM][Ac], and particularly for the better discrimination and quantification of halogen bonds (XB) vs induced force (IF), interior halogen bonds (IXB) vs exterior halogen bonds (EXB). Scheme 1 is the notation and structure of [BMIM][Ac] and iodine. The real pictures showing the color change are given in Scheme 2, while the proposed microscopically dynamic iodine sorption in [BMIM][Ac] is summarized in Scheme 3. Proportion of halogen bonds vs induced force, interior halogen bonds vs exterior halogen bonds at representative time points (140, 240, and 570 min) are shown in Scheme 4.

3.1. A direct color visualization for iodine sorption in [BMIM][Ac].

Scheme 2 shows a direct color change of iodine sorption in [BMIM][Ac]. The upper phase (supernatant) is the iodine solution with the cyclohexane as the solvent (ca. 0.2644 g, 0.384 g/L), showing a violet color. The lower phase (subnatant) is the neat [BMIM][Ac] (ca.1.9358 g), presenting a yellow color. Both supernatant and subnatant are loaded into a glass bottle (5 mL). The pictures in Scheme 2 show the color change of the sorption of iodine in [BMIM][Ac] with time from 0 h to 10 h with the increment of 1 h at room temperature. The color of supernatant (iodine phase) becomes shallow as the time elapses; the color of subnatant ([BMIM][Ac] phase) keeps almost unchanged.

A close inspection on Scheme 2 indicates that there is an occurrence of turning point at 2 h (120 min), in which a most drastic change in the color of supernatant iodine cyclohexane solution takes place. The huge color change before 120 min also indicates a fast iodine sorption rate, which may be due to a strong interaction between iodine and [BMIM][Ac]. Similarly, there might exist another turning point at 4 h (240 min), after which the color change of the supernatant iodine cyclohexane solution is minor, which maybe result from a weak interaction between

iodine and [BMIM][Ac]. Meanwhile, it also implies a slow iodine sorption rate. Between 120 min and 240 min, there might be a mixture of the strong and the weak interaction between iodine and [BMIM][Ac] in accompany with a moderate iodine sorption rate.

The two turning points (120 min and 240 min) divide the iodine sorption process into three zones. Zone 1 before 120 min; Zone 2 between 120 min and 240 min; and Zone 3 after 240 min. Zone 1 is attributed to a very strong I_2/IL interaction, leading to a fast iodine sorption rate and color change. Only a moderate I_2/IL interaction occurs in Zone 2, resulting in a moderate iodine sorption rate and color change. However, there are also two questions should be made clear.

The first question is: what is specifically the strong and weak I_2/IL interaction as mentioned above related to the zone-dividing speculation? Our previous study showed that the iodine would interact with ILs via two kinds of interactions: halogen bonds between the iodine (halogen atom, electrophilic species, electron acceptor, Lewis acid, XB donor) and the anion of ILs (electronegative species, electron donor, Lewis base, XB acceptor), and induced force ascribed to the high intrinsic electric filed of ILs and the highly-induced electron shell of iodine.[16] Generally, halogen bonds are stronger than induced force due to the relatively closer distance between the two atoms involving in halogen bonds than induced forces. Our previous investigation also concluded that the iodine sorption in ILs mainly via halogen bond (e.g., [BMIM][X] and [BMIM][TFO], X = Cl, Br, I) is more efficient than that mainly via induced force (e.g., [BMIM][BF_4], [BMIM][PF_4], [BMIM][Tf_2N], [BMIM][ClO_4]).[16] Thus, we interpret the strong I_2/IL interaction in Zone 1 as the halogen bonds, the weak I_2/IL interaction in Zone 3 as the induced force. I_2/IL interactions in Zone 3 include both halogen bonds and induced force.

The second question is: what is specifically the turning time point for the zone-dividing pattern related to the iodine sorption in [BMIM][Ac]? Deducing the turning points (120 min and 240 min) from the color change of the violet supernatant might be very rough. Furthermore, the color change is recorded every 1 h. Such a turning point-dividing way (by color change) and such a big time increment make us seek other more accurate methods to discriminate these two turning points. It would be anticipated that the turning points might be around 120 min and 240 min; the differences may not be very big. Next, we use in situ UV-vis spectroscopy (including normal and difference peak intensity, peak area as a function of time) in combination with two-dimensional correlation technique (including G-2D-COS, auto-MW2D-COS, PCMW2D-COS) to discriminate the turning points accurately, and then quantifying halogen bonds and induced force, interior halogen bonds and exterior halogen bonds, for I_2/IL system at some specific time points.

3.2. Dynamic process of iodine sorption in [BMIM][Ac].

The s-PCMW2D-COS shown in Fig. 8 indicates that 140 min is a turning point. It can also be clearly observed in as-PCMW2D-COS of Fig. 9 and 10, which corroborate the existence of turning point at 140 min. The color change of supernatant iodine cyclohexane solution also suggests a similar turning point at 120 min. It also implies that PCMW2D-COS is more accuracy than color visualization. The G-2D-COS discriminating ability (Fig. 5 and 6) is limited due to its averaging effect. The turning point might result from the iodine in the supernatant mainly interacts with [BMIM][Ac] via halogen bonds (including interior halogen bonds IXB and exterior halogen bonds EXB, which would be discussed later) before 140 min, while the induced force occurs after 140 min on the exterior of [BMIM][Ac].

Fig. 8 shows that another turning point in the s-PCMW2D-COS is at 240 min, after which the intensity change is negligible, before which, however, the change can not be neglected. Fig. 9 and 10 also support the existent of the second turning point at 240 min by as-PCMW2D-COS. The color change of supernatant iodine cyclohexane solution discussed above also suggests a similar turning point at 240 min, which again provides an evidence for the second turning point at 240 min by PCMW2D-COS. The G-2D-COS discriminating ability (Fig. 5 and 6) is limited due to its averaging effect. The change intensity after 240 min can be entirely ascribed to induced force on the [BMIM][Ac] exterior, while simultaneous induced force and halogen bonds would occur before 240 min on the [BMIM][Ac] exterior.

Thus, the dynamic process of iodine sorption in [BMIM][Ac] can be divided into three zones according to the above two discriminated dividing points (Fig. 2). The first 140 min belongs to Zone 1 as shown in Schemes 3a and 3b, where only halogen bonds occur (both interior halogen bonds in Scheme 3b and exterior halogen bonds in Scheme 3c). From 140 min to 240 min during Zone 2, halogen bonds (only including exterior halogen bonds) and induced force happen simultaneously on the [BMIM][Ac] exterior (Scheme 3d). In Zone 3 after 240 min, only exterior induced force takes place (Scheme 3e). Note that halogen bond includes interior and exterior, while induced force can only occur on the exterior.

Interestingly, there exists one minor turning point at 90 min in as-PCMW2D-COS of Fig. 10, which shows that Zone 1 could be divided into two subzones, i.e., Zone 1a (0-90 min in Scheme 3a) and Zone 1b (90-140 min in Scheme 3b). The change rate of Zone 1a is higher than that of Zone 1b, implying that Zone 1a involves a stronger form of halogen bonds (i.e., interior halogen bonds, Schemes 3a) while weaker halogen bonds (i.e., exterior halogen bonds, Schemes 3b) occur for Zone 1b. It is understandable because the first reacted iodine would penetrate into the [BMIM][Ac] interior via IXB before 90 min, which might in turn prevent the further entrance of iodine, hence an exterior halogen bonds after 90 min.

Another interesting finding is the existence of two minor turning points at 180 min and 200 min, as shown in as-PCMW2D-COS of Fig. 10. It indicates that Zone 2 can be divided into three subzones, i.e., Zone 2a (140 -180 min), Zone 2b (180-200 min), and Zone 2c (200-240 min). Also, s-PCMW2D-COS in Fig. 8 seems to show that 180 min and 200 min are two minor turning points in spite of less clearness than as-PCMW2D-COS in Fig. 10. Zone 2a, 2b and 2c correspond to most EXB, comparative and simultaneous EXB and exterior induced force, and most exterior induced force, respectively.

3.3. Microscopic explanation for the iodine dynamic sorption process in [BMIM][Ac].

The interaction contributing to iodine sorption in [BMIM][Ac] in Zone 1 is total halogen bonds, as shown in Schemes 3b and 3c. The entire halogen bonds in Zone 1 indicate that interaction

This journal is © The Royal Society of Chemistry [year]

between iodine and [BMIM][Ac] is the strongest, which prefers to occur first. It is possibly the iodine-anion halogen-bonding interaction because of a higher electrophilicity (a better XB donor) of iodine atom and a higher electronegativity (a better XB acceptor) of the acetate anion of [BMIM][Ac]. After this zone (after 140 min), [BMIM][Ac] might also interact with other iodine molecules via a less strong interaction (i.e., induced force), hence a less intensity change in Fig. 1, 2 and 7 after 140 min. The change in peak area also corroborates the same conjecture of the occurrence of a very strong I_2/IL interaction before 140 min. Specifically, this halogen-bonding interaction between I_2 and [BMIM][Ac] is not negligible until 200 min, as shown by the turning point in Fig. 10, which will be explained later. The strong halogen-bonding interaction might also induce a quick color change of iodine cyclohexane solution in the corresponding time period, as shown in Scheme 2. Owning to the higher strength of halogen bonds, a robust iodine sorption can be seen for many ILs to capture I_2.[16] Our previous iodine entrapment experiments also suggested that the initial iodine sorption rate by ILs is faster than that of afterwards time period, particularly for those ILs with a higher halogen bonds donating ability (e.g., [BMIM][Br]). On the other hand, removing this part of iodine would be very difficult, suggesting a better efficiency to reliably store radioactive iodine.[16].

Specifically, Zone 1 is divided into two subzones by a minor turning point at 90 min. The iodine is first drawn by [BMIM][Ac] into its interior via halogen bonds during the period before 90 min. Our previous study also reported that the strong halogen bonds would draw iodine into the interior of ILs.[16] The interesting thing is that they would form a more stable complex and a more viscous product. The stabilization of iodine by [BMIM][Ac] has been supported by nitrogen sweeping experiment.[16] The more viscous product could be visualized by adding some iodine solid power directly into the [BMIM][Ac]. Both reasons might prevent other iodine penetrate into the interior of the [BMIM][Ac], rather stays on the exterior of [BMIM][Ac] after 90 min, in spite of the same type of halogen bonds only with a very slightly less strength. It could be evidenced by the dividing point at 90 min (as-PCMW2D-COS of Fig. 10). In order to further corroborate this idea, we also conducted additional experiment by placing [BMIM][Ac] (0.5 mm height) on the bottom of ATR-cell and then cover it by iodine cyclohexane solution (1 mm height). Results show that the IR spectra of subnatant [BMIM][Ac] keep almost unchanged. It indicates that the iodine would not penetrate into the bottom of [BMIM][Ac], i.e., subinterior of IL phase as shown in Scheme 3. It also suggests that [BMIM][Ac]/I_2 complex would hinder a further penetration of iodine into the [BMIM][Ac] interior, which would in turn favor halogen-bonded iodine staying on the [BMIM][Ac] exterior to some extent. The proportion of exterior halogen bonds is found to be very less than that of interior halogen bonds, which we would discuss in the quantification section.

Zone 3 is the process of iodine sorption via only induced force on the exterior of [BMIM][Ac] as shown in Scheme 3e. The turning point 240 min can be clearly corroborated in the as-PCMW2D-COS (Fig. 10), roughly determined in the s-PCMW2D-COS (Fig. 8). Interestingly, this turning point to divide halogen bonds and induced force could also be justified by only eye visualization on the supernatant color change as shown in Scheme 2. In this process, iodine only interacts with the exterior of [BMIM][Ac] via induced force, which is weaker than halogen bonds in Zone 1, and therefore the already halogen-bonded [BMIM][Ac] in Zone 1 is not affected by the iodine sorption in this zone. The possible reason might be due to the reach of halogen-bonding accepting limit after 240 min. The absorbed halogen-bonded iodine prohibits [BMIM][Ac] to absorb more iodine via halogen bonds due to the full loading of iodine on the halogen-bonding accepting sites of [BMIM][Ac]. Other reasons could be the relatively high viscosity of neat [BMIM][Ac], and possibly a higher viscosity of [BMIM][Ac]/I_2 complex. Also note that there is no mechanic mixing or stirring device in the whole process, deterring again the iodine from percolating interior of the [BMIM][Ac] sample, rather staying on the exterior of [BMIM][Ac]. The UV spectra of the peak intensities and area thus remain almost unchanged (Fig. 1, 2, 3, 4, 7); all the bands varying in this zone can thus be due to the iodine absorbed on the exterior [BMIM][Ac] via induced force. Induced force is weaker than halogen bonds, thus iodine sorption in this zone is minor and slow, which can be easy removed to some extent. It is consistent with our previous report that iodine is adsorbed on the exterior of ILs with less XB accepting ability (e.g., [BMIM][ClO_4]) and can thus be easily removed.[16] A slow absorption rate could also be witnessed for the iodine sorption by many ILs in this zone.[16]

Zone 2 from 140 to 240 min is a transition zone with three subzones shown in Fig. 10 and Scheme 3. The main feature is the sorption of iodine via simultaneous halogen bonds and induced force. The as-PCMW2D-COS in Fig. 9 and 10, s-PCMW2D-COS in Fig. 8, and supernatant color change in Scheme 2 all support the existence of the second zone. In this zone, the strongest interaction (interior halogen bonds) is totally depleted; the stronger interaction (exterior halogen bonds) is almost exhausted; the weak interaction (i.e., exterior induced force) begins to emerge. Thus, the remaining exterior halogen bonds and exterior induced force are combined to play a role in determining iodine sorption in [BMIM][Ac] simultaneously. Note that, in this zone, all the iodine is absorbed on the exterior of [BMIM][Ac] due to the occupation of IL by iodine via interior halogen bonds as discussed above. Particularly, the existence of the three subzones in Zone 2 (Zone 2a, Zone 2b, and Zone 2c) is evidenced by the more accurate as-PCMW2D-COS in Fig. 10, which would be discussed below.

From 140 to 180 min (Zone 2a), the exterior halogen bonds dominate the iodine sorption (compared with Zone 1), and only a slight induced force takes place. In general, Zone 2a resembles Zone 1. In Zone 2a, there still exist some un-halogen-bonded acetate anions that the iodine needs; the interaction is also strong although fewer anions participate in the halogen bonds with the supernatant iodine than that in Zone 1. Thus, in this subzone, alternation of intensity also exists while with a slower rate than that in Zone 1 (Fig. 1, 2, 3, 4, 7). Still, the halogen bonds in this subzone stay on the exterior of [BMIM][Ac]. From 180 to 200 min (Zone 2b), both exterior halogen bonds and induced force are contributing to the iodine sorption. In Zone 2b, very fewer acetate anions are available to uptake supernatant iodine by halogen-

bonding interactions. Thus, the electron shell of iodine is induced by [BMIM][Ac] with high intrinsic electric filed, which could be corroborated by the zone from 180 to 200 min in Fig. 10. From 200 to 240 min (Zone 2c), the (exterior) induced force takes up the most part of the iodine sorption while (exterior) halogen bonds is few. In general, Zone 2c resembles Zone 3. In Zone 2c, almost all of the anions of IL that are able to halogen-bonded with iodine have already been interacted; only negligible acetate anions to absorb iodine via exterior halogen bonds. The most possible interaction for supernatant iodine to be absorbed on [BMIM][Ac] is the induced force.

3.4. Quantifying halogen bonds and induced force.

Conclusions drawn above by s-PCMW2D-COS (Fig. 8), as-PCMW2D-COS (Fig. 9 and 10), and color change (Scheme 2) suggest that 240 min is a turning point, after which iodine is absorbed only on the exterior of [BMIM][Ac] via induced force; another turning point is discriminated at 140 min, before which iodine is absorbed only into [BMIM][Ac] via halogen bonds. Considering the two turning points, the dynamic process of iodine sorption by [BMIM][Ac] could be described as below. At the first 140 min, only (interior and exterior) halogen bonds occur. From 140 to 240 min, (exterior) halogen bonds and (exterior) induced force occur simultaneously. After 240 min, only (exterior) induced force occurs. Specifically, Zone 1 consists of two subzones, i.e., Zone 1a (before 90 min) and Zone 1b (90-140 min), corresponding to interior and exterior halogen bonds, respectively. Zone 2 is constituted of three subzones, i.e., Zone 2a (140-180 min), Zone 2b (180-200 min), and Zone 2c (200-240 min), with (exterior) halogen bonds taking up the most part, about one half, and small part of the total iodine sorption, respectively.

Based on the clarification of the dynamic iodine sorption process, we quantify the halogen bonds vs induced force of iodine sorption in [BMIM][Ac] by combining with its UV-vis spectroscopy intensity. The intensity (Fig. 1a and 1b) derived from UV-vis spectroscopy directly corresponds to the concentration of iodine cyclohexane solution according to the Beer–Lambert law, in which the molar absorptivity is estimated as 3.441 $L \cdot g^{-1} \cdot mol^{-1}$.[16] By using the UV-vis spectroscopy, we also measured molar absorption coefficient for many kinds of ILs.[70] However, here we do not use the normal absorbance intensity developed from UV-vis spectroscopy or the real concentration derived form the Beer-Lambert law. Rather, we select the absorbance from the difference UV-vis spectroscopy (Fig. 2a and 2b), which could provide the change of concentration of iodine at the cyclohexane solution more directly and simply. All of the data are positive after ignoring the sign of UV-vis difference spectroscopy. Therefore, the change of iodine sorption relative capacity at 0, 140 (the first turning point), 180, 200, 240 (the second turning point), and 570 min could be derived as 0 (A_{0min}), 1.36 (A_{140min}), 1.43 (A_{180min}), 1.46 (A_{200min}), 1.51 (A_{240min}), 1.59 (A_{570min}), respectively.

First, we quantify the proportion of halogen bonds and induced force within 570 min. The components of iodine sorption in [BMIM][Ac] via halogen bonds include three categories as shown in Eq. 1: (i) in Zone 1, the relative content of halogen bonds is ca. 1.36 by subtracting A_{140min} from A_{0min}; (ii) in Zone 2a, it is ca. 0.07 by subtracting A_{180min} from A_{140min} after assuming a totally halogen bonds contribution; (iii) in Zone 2b, it is ca. 0.015, half of the difference between A_{200min} and A_{180min}, based on the assumption that the halogen bonds and induced force are comparable in this subzone. After considering all the three kinds of contribution, halogen bonds are calculated as 1.445. The overall contribution of induced force could be calculated with Eq. 2. For a better understanding, we also divide it into three parts: (Ⅰ) from Zone 3, the relative content of induced force is ca. 0.08, i.e., the difference between A_{570min} and A_{240min}; (Ⅱ) from Zone 2c, it is ca. 0.05, by A_{240min} minus A_{200min}, on the basis of the premise of a totally induced force contribution despite a almost all pattern; (Ⅲ) from Zone 2b, it is ca. 0.015, which is the same situation discussed in (iii). The sum of the three species (0.08, 0.05, and 0.015) would result in 0.145 all together for the overall induced force within 570 min. Therefore, the proportion of halogen bonds and induced force resulting in iodine sorption by [BMIM][Ac] within 570 min could be derived approximately as 91% and 9% (Scheme 4c), according to Eq. 3 and Eq. 4, respectively.

Then, the relative content of halogen bonds and induced force within 240 min would be quantified by refereeing to the methods as discussed above within 570 min. Similar to 570 min, the constituents of halogen bonds within 240 min can also be divided into three compositions as shown in Eq. 5. A more close inspection would find that the content of halogen bonds within 240 min is the same as that of 570 min. However, the amount of induced force resulting in the iodine sorption in [BMIM][Ac] within 240 min is different from that within 570 min. Specifically, the content of induced force during Zone 3 (ca. 0.08 in Ⅰ) is excluded within 240 min (Eq. 6) while included within 570 min (Eq. 2). Adding the contribution of induced force from Zone 2c (ca. 0.05 in Ⅱ) and Zone 2b (ca. 0.015 in Ⅲ) would obtain the overall induced force within 240 min, i.e., 0.065. After considering the relative content of halogen bonds (1.445) and induce force (0.065), the proportion can be estimated as 96% and 4%, respectively (as shown in Scheme 4b), by refereeing to the similar equations for (Eq. 3 and 4 for the time region within 570 min) the halogen bonds- and induced force-proportion quantification.

Another time point at 140 min is also selected to analyze the proportion of halogen bonds and induced force due to the first turning point at 140 min, which stands for a representative time point for the halogen bonds and induced force determination. In this case, the overall halogen bonds and induced force caused for the iodine sorption in [BMIM][Ac] are more easy to be justified owning to a simpler constituents. Namely, only Zone 1, i.e., ca. 1.36 in (i), is included in the content of halogen bonds within 140 min as shown in Eq. 7. Nevertheless, there is no induced force included in the same time region (Eq. 8). Thus, the proportion of halogen bonds and induced force could be determined quite simply, i.e., 100% and 0%, respectively, as shown in Scheme 4a. The most important feature of iodine sorption in [BMIM][Ac] is that halogen bonds dominate the entrapment process during a long-term exposure (e.g., 91% within 570 min, 96 within 240 min), particularly a short-term exposure (e.g., 100% within 140 min), while the contribution of induced force for iodine sorption in [BMIM][Ac] is minor (9% at most). It is highly consistent with our previous work on selecting ILs ([BMIM][Ac]) to capture iodine mainly via halogen bonds due to a good halogen-bonding

This journal is © The Royal Society of Chemistry [year]

accepting ability of the acetate anion.[16]

3.5. Quantifying interior halogen bonds (IXB) and exterior halogen bonds (EXB).

In the above quantification of halogen bonds and induced force, induced force contributes to an exterior sorption of iodine due to its weaker strength while halogen bonds leads to both an interior (IXB) and an exterior (EXB) iodine sorption. We cannot distinguish exterior or interior induced force, because induced force only includes exterior pattern. However, in terms of halogen bonds, it contains interior halogen bonds and exterior halogen bonds. In terms of determining the proportion of halogen bonds and induced force, we do not differentiate interior or exterior halogen bonds because it is not necessary. The indiscrimination of interior or exterior halogen bonds would make the quantification process simpler and more convenient. Below, we tend to make a discrimination of interior and exterior halogen bonds and then quantify them by choosing some representative time point (particularly at the two turning points and the experiment-ending time point). Before the quantification, we should determine the intensity of the first turning point at 90 min discriminating interior and exterior halogen bonds, A_{90min} = 1.16, which is derived from the raw data directly.

We first quantify the proportion of interior and exterior halogen bonds within 240 min. The interior halogen bonds only occur before 90 min, thus the overall content could be easily determined as ca. 1.16 in Zone 1a (Eq. 9). However, the components of exterior halogen bonds include three species according to Eq. 10. The first species comes from Zone 1b, the difference between A_{140min} and A_{90min} (ca. 0.20); the second part is the same as that of (ii) as discussed above, which is included in Zone 2a, ca. 0.07; the third category is also equivalent to that of (iii) as discussed above in Zone 2b around 0.015. The sum of the three types' value (0.20, 0.07, and 0.015) is 0.285, the overall exterior halogen bonds needed for the iodine sorption in [BMIM][Ac]. Therefore, the proportion of interior halogen bonds (80%, Scheme 4e) within 240 min could be derived after dividing 1.16 by the sum of 0.20 and 0.285, i.e., 1.445 (Eq. 11). Similarly, by utilizing Eq. 12, the proportion of exterior halogen bonds (20%, Scheme 4e) within 240 min could also be obtained. Obviously, most (80%) of the iodine sorption takes place via the way of interior halogen bonds within 240 min. Then, the subsequent exterior halogen bonds are inhibited (i.e., 20%) due to some physical (e.g., no stirring or mixing behavior, higher viscosity after sorption) or chemical reasons (e.g., weaker halogen-bonding accepting ability of the acetate anion) as suggested above.

When the time point is set as 140 min, the proportion of interior and exterior halogen bonds would vary to some extent. As to the content of interior halogen bonds, it keeps the same with that within 240 min, ca. 1.16 in Zone 1a (Eq. 13). In terms of exterior halogen bonds within 140 min, its content changes slightly when compared with that of 240 min (Eq. 14). Specifically, only the first component (ca. 0.20 in Zone 1b) of exterior halogen bonds discussed above in 240 min remains to 140 min, while the other two components (Zone 2a and Zone 2b) are not included. Thus, the overall content of exterior halogen bonds within 140 min is only ca. 0.20. In this way, the proportion of interior and exterior of halogen bonds could be obtained as 85% and 15%, respectively (Scheme 4d). In this case, the contribution of interior halogen bonds is also higher than that of exterior halogen bonds. If we choose the experiment-ending time point, i.e., 570 min, the proportion of interior and exterior halogen bonds could also be secured. In the case within 570 min, it would keep the same as that within 240 min, because there are no form of halogen bonds involved in the iodine sorption after 240 min. Namely, the proportion of interior and exterior halogen bonds within 570 min is also 80% and 20%, respectively.

In all the three cases (140 min, 240 min, 570 min), the function of interior halogen bonds is higher than that of exterior halogen bonds resulting in the iodine sorption in [BMIM][Ac]. It suggests that [BMIM][Ac] binds iodine mainly via halogen bonds into its interior rather than on the exterior. Our previous study also anticipated that it would take less time to reach maximum iodine sorption with stirring.[16] Another interesting finding is that the proportion increase (4% - 0% = 4% from Schemes 2a and 2b) of induced force from 140 min to 240 min is comparable to that (20% -15% = 5% from Schemes 2d and 2e) of exterior halogen bonds during the same time zone (Zone 2). It is consistent with our assumption of a simultaneous and comparable (exterior) halogen bonds and induced force in Zone 2 from 140 to 240 min as suggested above. Before 140 min (Zone 1), the interior halogen bonds are totally exhausted, and the exterior halogen bonds is almost depleted. In Zone 2, induced force would have a synergistic effect with the remaining exterior halogen bonds on the contribution of iodine sorption in [BMIM][Ac].

4. Conclusion

Here, we for the first time investigate the dynamic process of radioactive iodine sorption in a representative AcILs, [BMIM][Ac]. Furthermore, the halogen bonds (including interior and exterior types) and induced force (only owning a exterior form) resulting in iodine sorption in [BMIM][Ac] at some specific time point are discriminated and quantified.

Results show that the dynamic iodine sorption in [BMIM][Ac] could be divided into three zones. In Zone 1, only (interior and exterior) halogen bonds occur (the first 140 min). From 140 to 240 min, (exterior) halogen bonds and induced force occur simultaneously (Zone 2). After 240 min, only induced force occurs (Zone 3). Specifically, Zone 1 consists of two subzones, Zone 1a (before 90 min) and Zone 1b (90-140 min), corresponding to interior and exterior halogen bonds, respectively. Zone 2 is constituted of three subzones, Zone 2a (140-180 min), Zone 2b (180-200 min), and Zone 2c (200-240 min), with (exterior) halogen bonds taking up the most part, about one half, and a small part of the total iodine sorption, respectively. The proportion of halogen bonds and induced force resulting in iodine sorption by [BMIM][Ac] could be derived approximately as 100% and 0% within 140 min, 96% and 4% within 240 min, 91% and 9% within 570 min, respectively. Furthermore, the proportion of interior and exterior halogen bonds resulting in iodine sorption by [BMIM][Ac] could be derived approximately as 85% and 15% within 140 min, 80% and 20% within 240 min, 80% and 20% within 570 min, respectively.

These processes and quantification would provide insight into how the iodine is removed by [BMIM][Ac] in the form of sorption, and may motivate further experimental or theoretical

studies on the application of halogen bonds on removal of iodine by designing new types of ILs, particularly for those task-specific ILs tethering with amine, hydroxyl, unsaturated bond that assume to a good halogen-bonding acceptor for the halogen-bonding donor iodine. Note that although the halogen bonds and induced force have been discriminated in this paper, more work is still needed to make it clearer. Other kinds of ILs might also show a similar pattern, but is not the scope of this article here. Again, the external factors affecting the dynamic process and the quantification of halogen bonds and induced force are also our interest. In a word, we for the first time investigate the dynamic process of radioactive iodine sorption in [BMIM][Ac], and approximately quantify the halogen bonds vs induced force, interior vs exterior halogen bonds.

Author Information

Corresponding Author
*Tel.: +86-10-62514925. Fax: +86-10-62516444. E-mail: tcmu@chem.ruc.edu.cn.
The authors declare no competing financial interest.

Acknowledgement

This work was supported by the National Natural Science Foundation of China (21473252). We also thank ~~Professor~~ Morita (Division of Energy Science, EcoTopia Science Institute, Nagoya University, Furo-cho, Chigusa-ku, Nagoya 464-8603, Japan) and ~~Professor~~ Ozaki (Department of Chemistry, School of Science and Technology, Kwansei-Gakuin University, Sanda 669-1337, Japan) to help us via email to obtain PCMW2D-COS with the software 2D shige.

This journal is © The Royal Society of Chemistry [year]

$$A_{XB\text{-}570min} = (A_{140min} - A_{0min})_{Zone1} + (A_{180min} - A_{140min})_{Zone2a} + (A_{200min}/2 - A_{180min}/2)_{Zone2b} \quad (1)$$

$$A_{IF\text{-}570min} = (A_{570min} - A_{240min})_{Zone3} + (A_{240min} - A_{200min})_{Zone2c} + (A_{200min}/2 - A_{180min}/2)_{Zone2b} \quad (2)$$

$$P_{XB\text{-}570min} = A_{XB\text{-}570min} / (A_{XB\text{-}570min} + A_{IF\text{-}570min}) \quad (3)$$

$$P_{IF\text{-}570min} = A_{IF\text{-}570min} / (A_{XB\text{-}570min} + A_{IF\text{-}570min}) \quad (4)$$

$$A_{XB\text{-}240min} = (A_{140min} - A_{0min})_{Zone1} + (A_{180min} - A_{140min})_{Zone2a} + (A_{200min}/2 - A_{180min}/2)_{Zone2b} \quad (5)$$

$$A_{IF\text{-}240min} = (A_{240min} - A_{200min})_{Zone2c} + (A_{200min}/2 - A_{180min}/2)_{Zone2b} \quad (6)$$

$$A_{XB\text{-}140min} = (A_{140min} - A_{0min})_{Zone1} \quad (7)$$

$$A_{IF\text{-}140min} = 0 \quad (8)$$

$$A_{IXB\text{-}240min} = (A_{90min} - A_{0min})_{Zone1a} \quad (9)$$

$$A_{EXB\text{-}240min} = (A_{140min} - A_{90min})_{Zone1b} + (A_{180min} - A_{140min})_{Zone2a} + (A_{200min}/2 - A_{180min}/2)_{Zone2b} \quad (10)$$

$$P_{IXB\text{-}240min} = A_{IXB\text{-}240min}/(A_{IXB\text{-}240min} + A_{EXB\text{-}240min}) \quad (11)$$

$$P_{EXB\text{-}240min} = A_{EXB\text{-}240min}/(A_{IXB\text{-}240min} + A_{EXB\text{-}240min}) \quad (12)$$

$$A_{IXB\text{-}140min} = (A_{90min} - A_{0min})_{Zone1a} \quad (13)$$

$$A_{EXB\text{-}140min} = (A_{140min} - A_{90min})_{Zone1b} \quad (14)$$

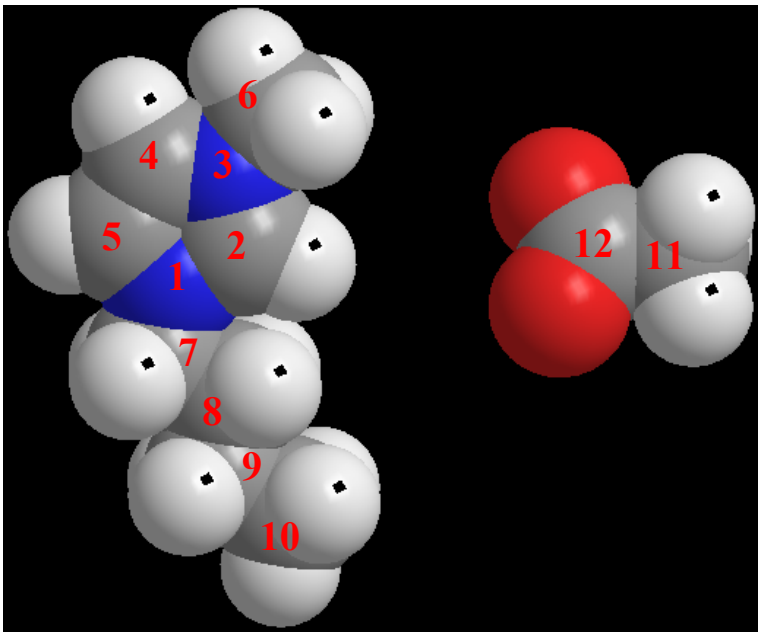

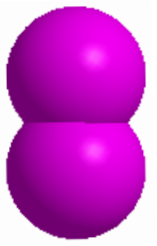

(c)

Scheme 1. Chemical structure and notation of [BMIM][Ac] and iodine I_2: cation 1-butyl-3-methyl-imidazolium [BMIM] (a), anion acetate [Ac] (b), and elemental iodine (c). The relationship between the kinds of atom and the 5 color of atom are listed below: C (grey), N (blue), O (red), H (white), I (violet).

This journal is © The Royal Society of Chemistry [year]

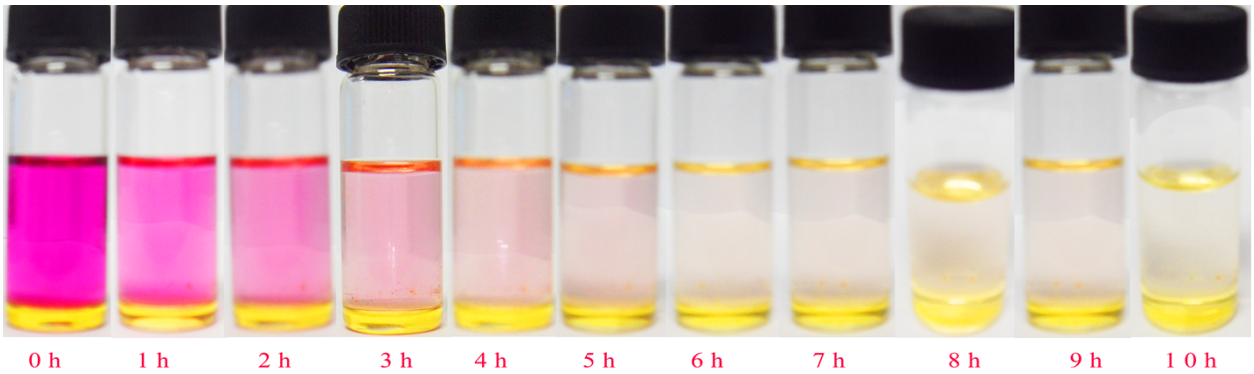

Scheme 2. Color of iodine cyclohexane solution in [BMIM][Ac] as a function of time from 0 h to 10 h with the increment 1 h at the room temperature ca. 20 ^{o}C. The upper phase is the iodine cyclohexane solution. The lower phase is [BMIM][Ac], showing a yellow color. The seemingly yellow color in the top surface inner the glass bottle is not a phase but only a light reflection or refraction at the experimental condition. The picture is taken separately for each one by using a same white paper as the substrate, and then combined together.

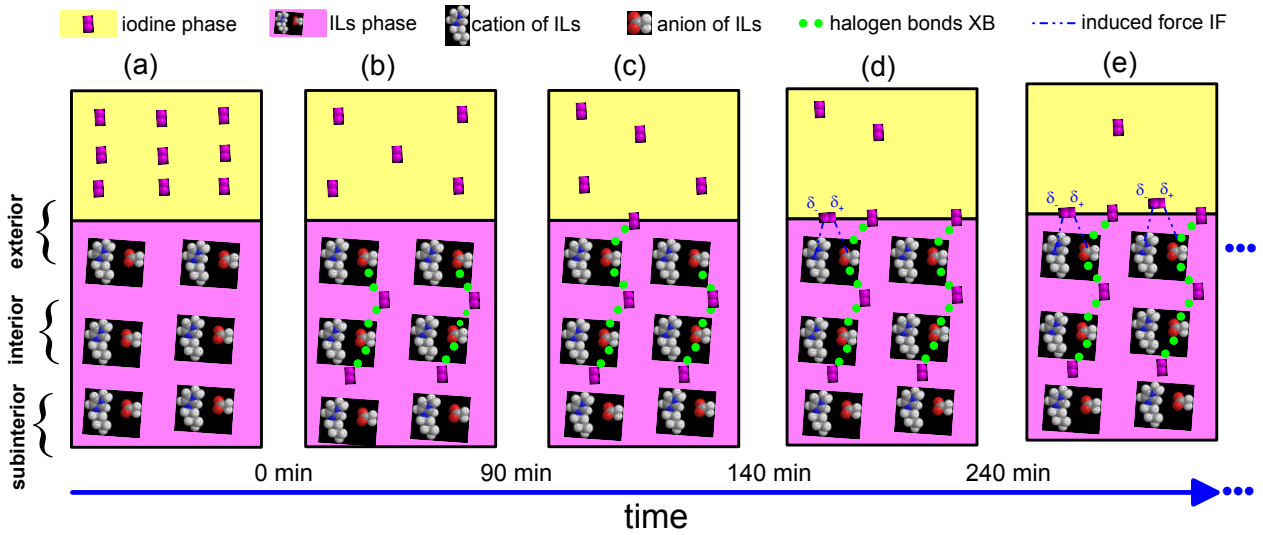

Scheme 3. Proposed dynamic process of iodine sorption in [BMIM][Ac] as a function of time: begin at 0 min (a), only interior halogen bonds before 90 min (b), only exterior halogen bonds between 90 min and 140 min (c), simultaneous exterior halogen bonds and induced force between 140 min and 240 min (d), only induced force after 240 min (e). Exterior refers to the interface layer between [BMIM][Ac] phase and iodine phase; Interior represents the layer below the interface layer between [BMIM][Ac] phase and iodine phase; Subinterior means all the area below interior until the bottom surface of [BMIM][Ac] phase. Iodine phase (upper phase) is the iodine cyclohexane solution; ILs phase (lower phase) is the pure ILs.

This journal is © The Royal Society of Chemistry [year]

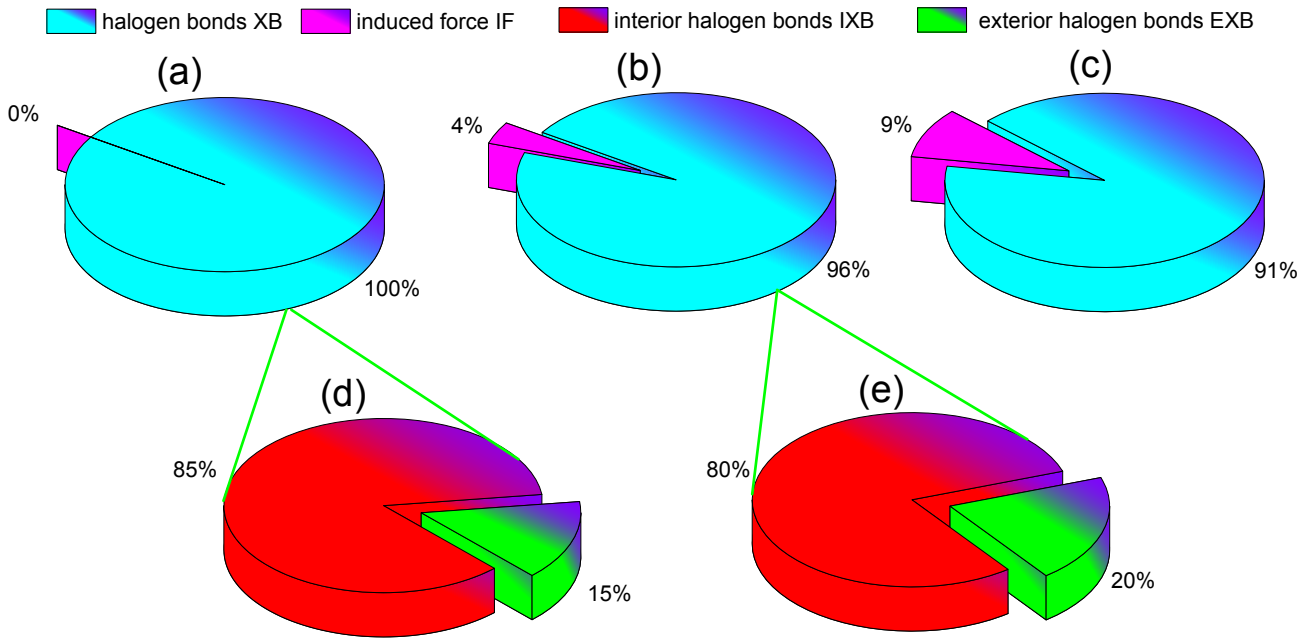

Scheme 4. Proportion of halogen bonds and induced force for the iodine sorption in [BMIM][Ac] as a function of time at 140 min (a), at 240 min (b), at 570 min (c), and proportion of interior (IXB) and exterior halogen bonds (EXB) within the overall halogen bonds at 140 min (d), at 240 min (e), corresponding respectively to the components of halogen bonds in (a) and (b).

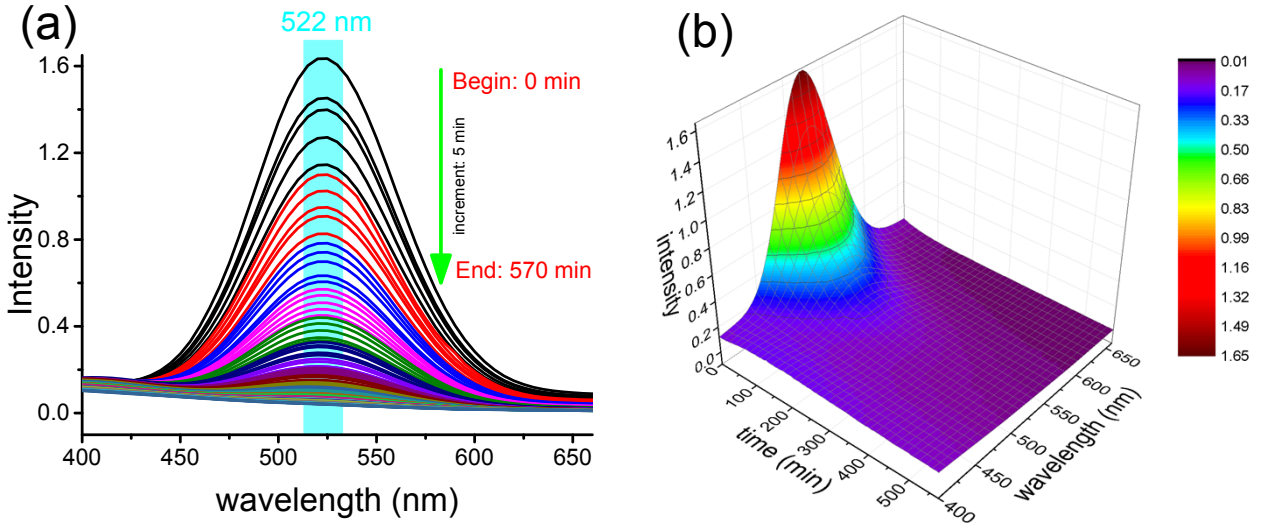

Fig. 1. UV-vis spectroscopy peak intensity of iodine cyclohexane solution in the upper phase for the iodine sorption in [BMIM][Ac] as a function of time from 0 min to 570 min with the increment 5 min: linear (a) and stereoscopic (b) 5 presentation.

This journal is © The Royal Society of Chemistry [year]

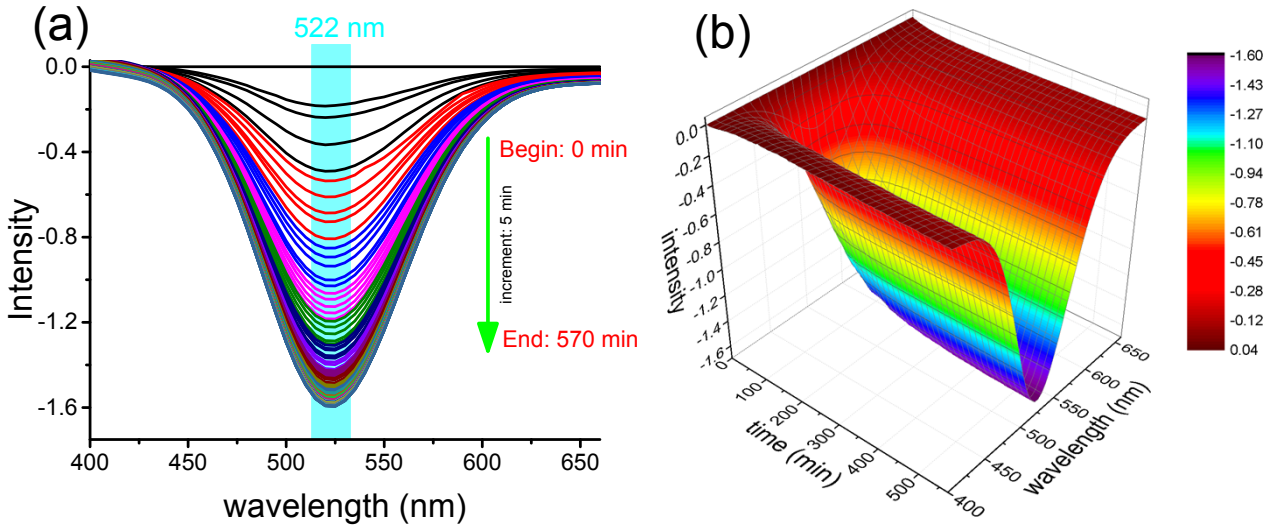

Fig. 2. Difference UV-vis spectroscopy peak intensity of iodine cyclohexane solution in the upper phase for the iodine sorption in [BMIM][Ac] as a function of time from 0 min to 570 min with the increment 5 min: linear (a) and stereoscopic (b) presentation. The difference spectra are obtained by subtracting the reference spectrum at 0 min from the whole spectra.

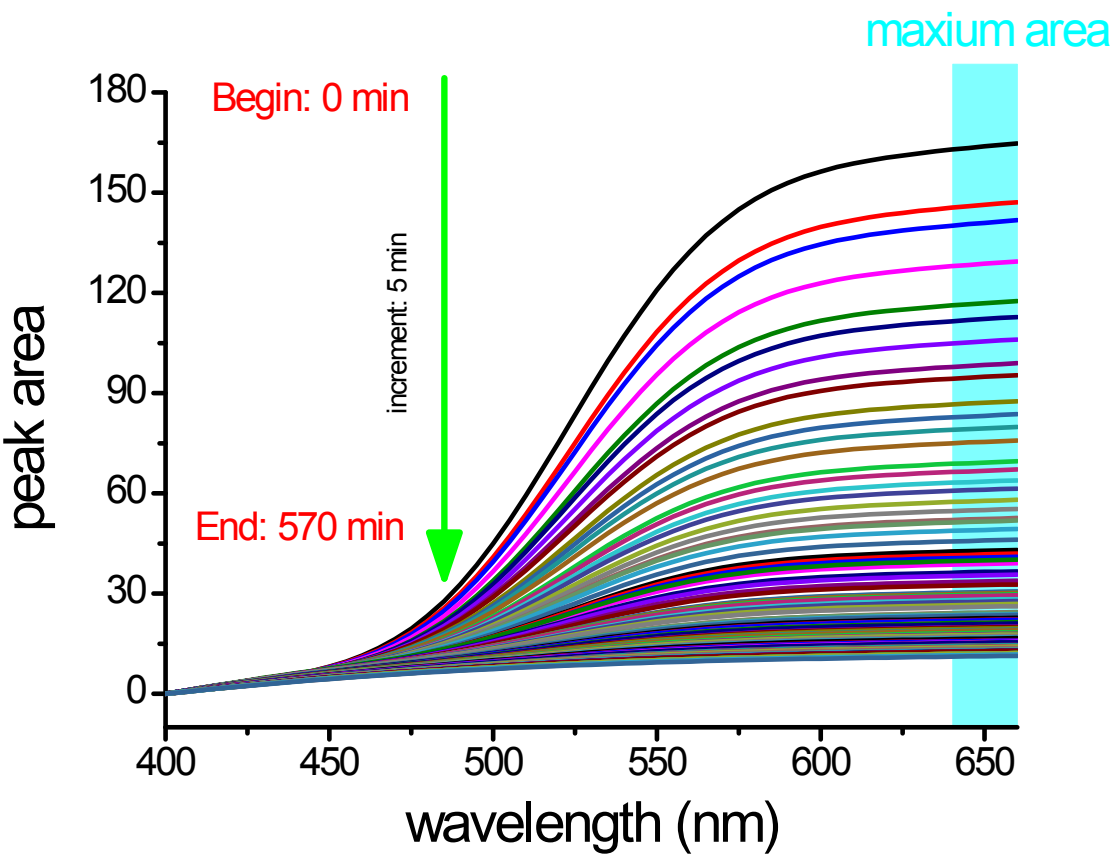

Fig. 3. UV-vis spectroscopy peak area of iodine cyclohexane solution in the upper phase for the iodine sorption in [BMIM][Ac] as a function of time from 0 min to 570 min with the increment 5 min: linear presentation.

5

This journal is © The Royal Society of Chemistry [year]

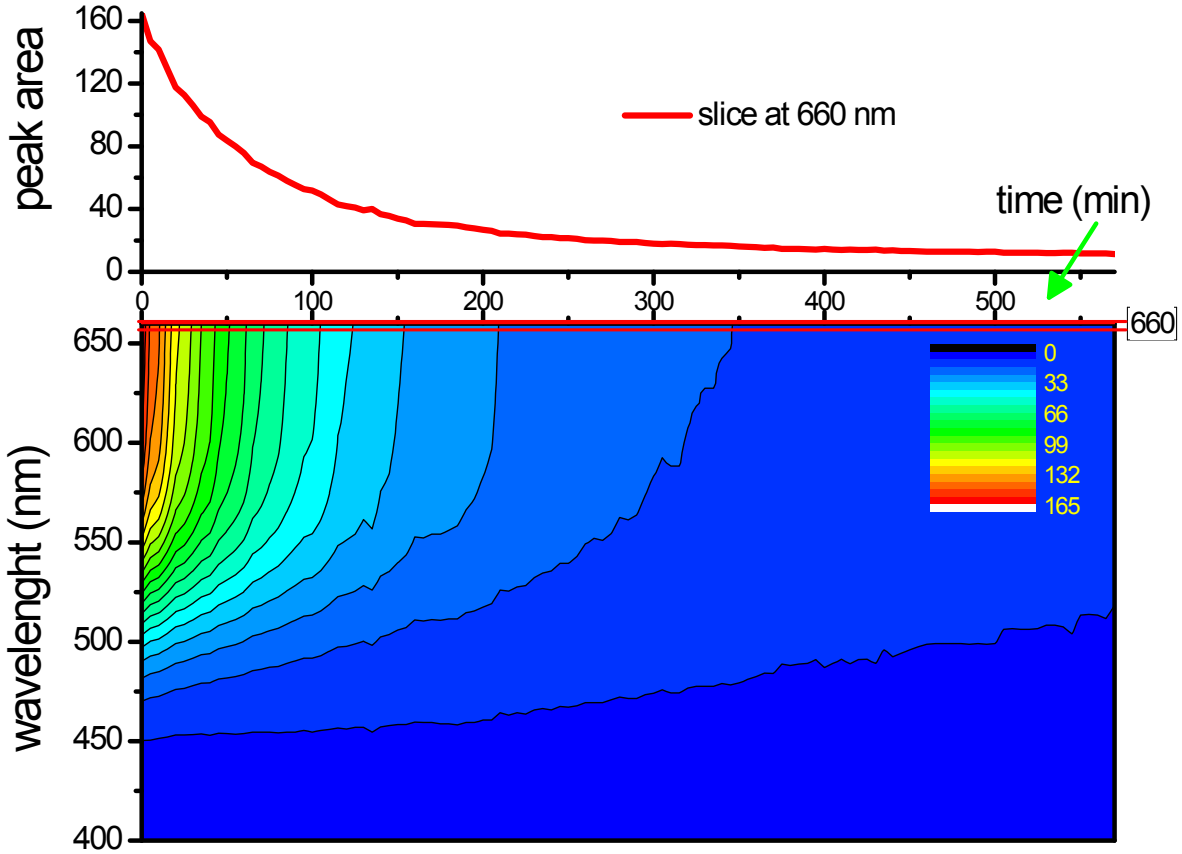

Fig. 4. UV-vis spectroscopy peak area of iodine cyclohexane solution in the upper phase for the iodine sorption in [BMIM][Ac] as a function of time from 0 min to 570 min with the increment 5 min: slice spectrum at 660 min (up) stereoscopic presentation with profile (down).

5

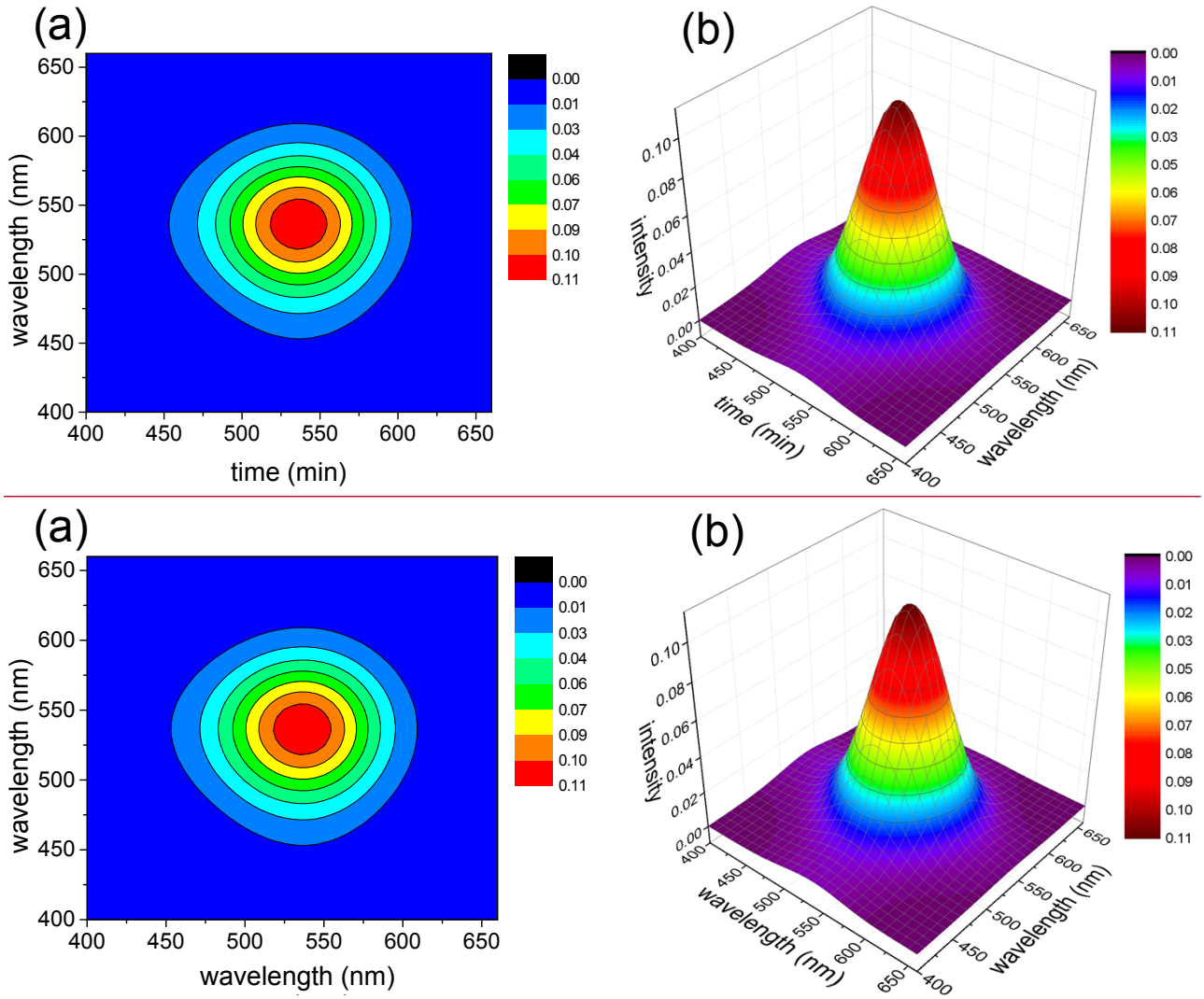

Fig. 5. s-G-2D-COS UV-vis spectroscopy peak intensity for the iodine sorption in [BMIM][Ac] as a function of 5 time from 0 min to 570 min with the increment 5 min: planar (a) and stereoscopic (b) presentation.

This journal is © The Royal Society of Chemistry [year]

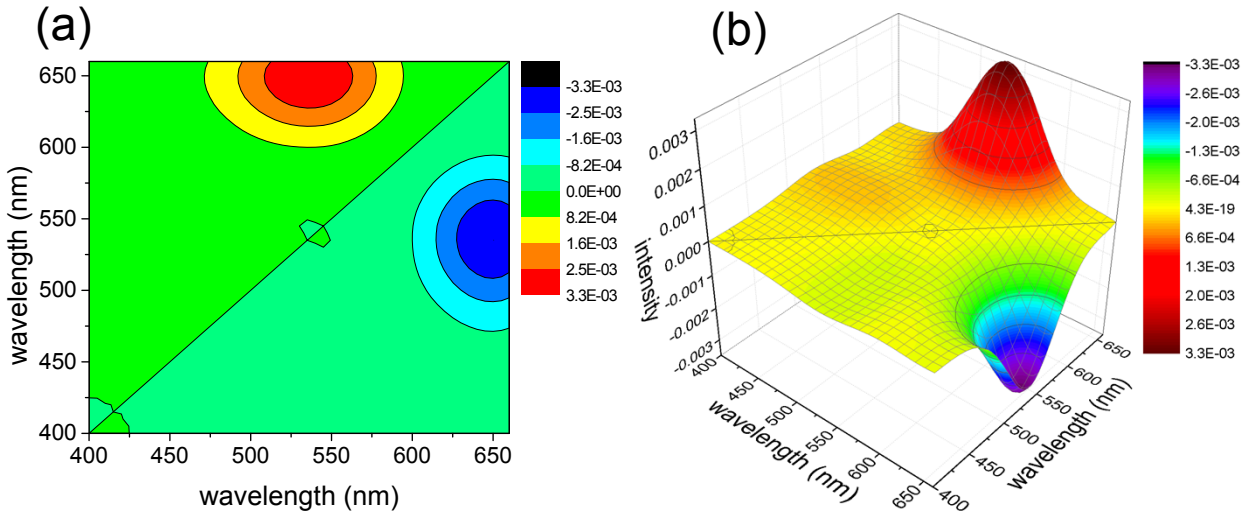

Fig. 6. as-G-2D-COS UV-vis spectroscopy peak intensity for the iodine sorption in [BMIM][Ac] as a function of time from 0 min to 570 min with the increment 5 min: planar (a) and stereoscopic (b) presentation.

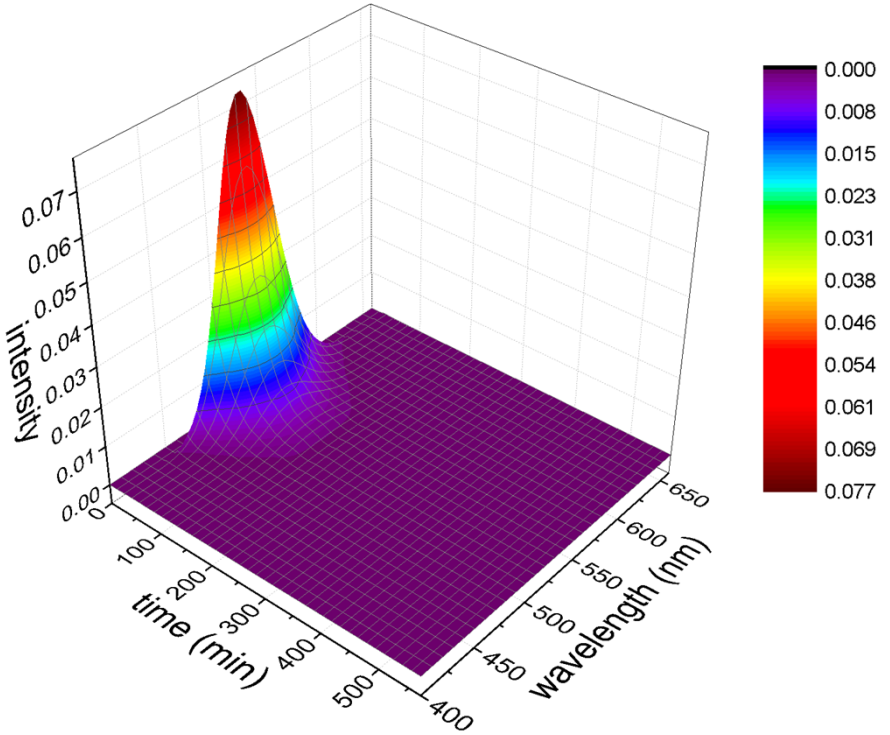

Fig. 7. auto-MW2D-COS UV-vis spectroscopy peak intensity for the iodine sorption in [BMIM][Ac] as a function of time from 0 min to 570 min with the increment 5 min: stereoscopic presentation.

5

This journal is © The Royal Society of Chemistry [year]

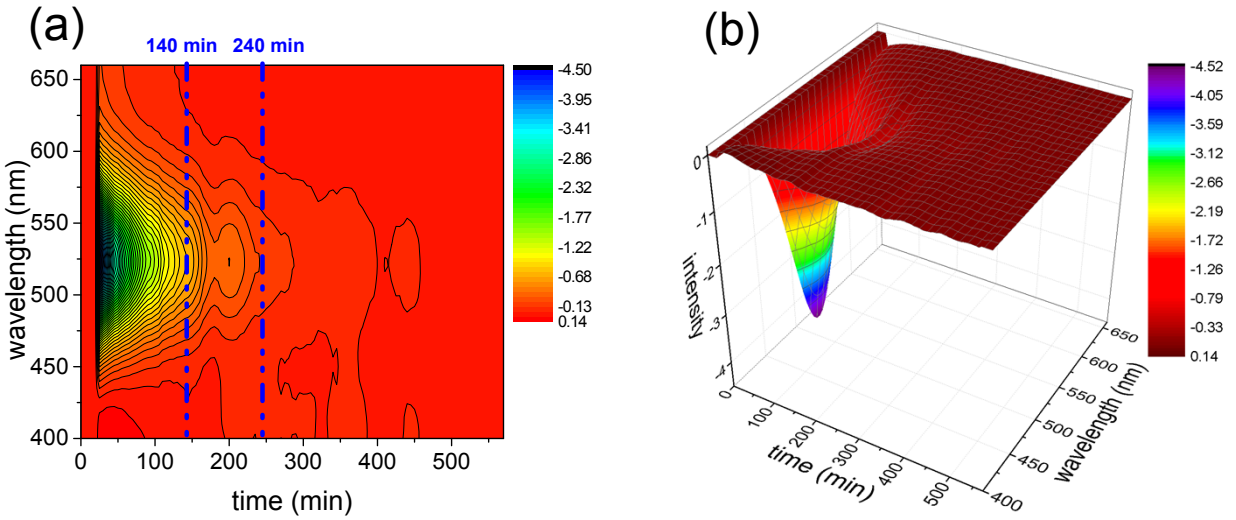

Fig. 8. s-PCMW2D-COS UV-vis spectroscopy peak intensity for the dynamic process of iodine sorption in [BMIM][Ac] as a function of time from 0 min to 570 min with the increment 5 min: planar (a) and stereoscopic (b) 5 presentation.

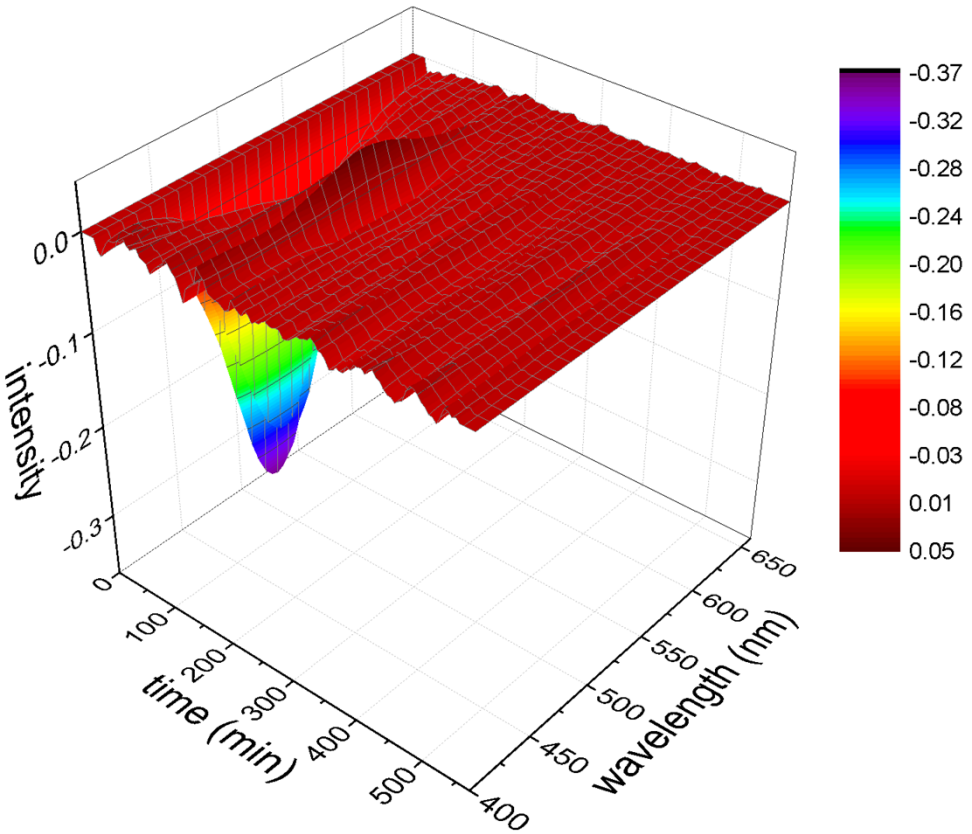

Fig. 9. as-PCMW2D-COS UV-vis spectroscopy peak intensity for the iodine sorption in [BMIM][Ac] as a function of time from 0 min to 570 min with the increment 5 min: stereoscopic presentation.

This journal is © The Royal Society of Chemistry [year]

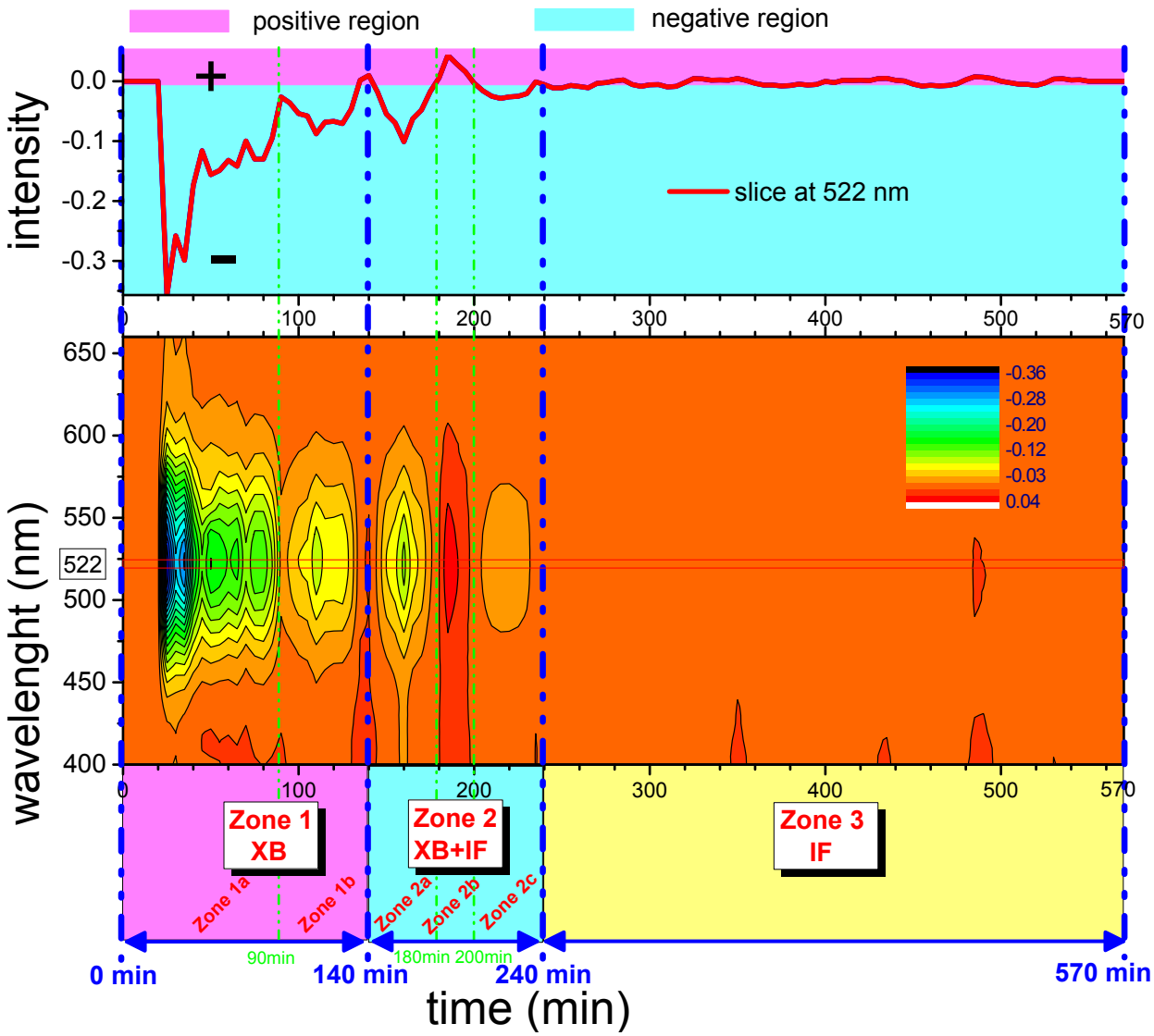

Fig. 10. as-PCMW2D-COS UV-vis spectroscopy peak intensity for the iodine sorption in [BMIM][Ac] as a function of time from 0 min to 570 min with the increment 5 min: slice spectrum at 522 nm (up) and planar presentation with profile (down). The thick blue and thin green line are the dividing point of zones and subzones, discriminated with the Arabic numerals (i.e., 1, 2, 3) and the English letters (i.e., a, b, c), respectively. XB and IF are the abbreviations for halogen bonds and induced force, respectively.

References

1. S. Xu, S. P. Freeman, X. Hou, A. Watanabe, K. Yamaguchi and L. Zhang, Environ. Sci. Technol., 2013, **47**, 10851-10859.
2. X. Hou, C. Fogh, J. Kucera, K. G. Andersson, H. Dahlgaard and S. P. Nielsen, Sci. Total. Environ., 2003, **308**, 97-109.
3. J. P. Bleuer, Y. I. Averkin and T. Abelin, Environ. Health Persp., 1997, **105**, 1483.
4. E. Ostroumova, A. Rozhko, M. Hatch, K. Furukawa, O. Polyanskaya, R. J. McConnell, E. Nadyrov, S. Petrenko, G. Romanov and V. Yauseyenka, Environ. Health Persp., 2013, **121**, 865.
5. K. W. Chapman, P. J. Chupas and T. M. Nenoff, J. Am. Chem. Soc., 2010, **132**, 8897-8899.
6. D. F. Sava, M. A. Rodriguez, K. W. Chapman, P. J. Chupas, J. A. Greathouse, P. S. Crozier and T. M. Nenoff, J. Am. Chem. Soc., 2011, **133**, 12398-12401.
7. C. Falaise, C. Volkringer, J. Facqueur, T. Bousquet, L. Gasnot and T. Loiseau, Chem. Commun., 2013, **49**, 10320-10322.
8. M.-H. Zeng, Q.-X. Wang, Y.-X. Tan, S. Hu, H.-X. Zhao, L.-S. Long and M. Kurmoo, J. Am. Chem. Soc., 2010, **132**, 2561-2563.
9. Q.-K. Liu, J.-P. Ma and Y.-B. Dong, Chem. Commun., 2011, **47**, 7185-7187.
10. P.-S. Huang, C.-H. Kuo, C.-C. Hsieh and Y.-C. Horng, Chem. Commun., 2012, **48**, 3227-3229.
11. X. Liu, A. Sigen, Y. Zhang, Z. Li, H. Xia, M. Xue and Y. Mu, Chem. Commun., 2014.
12. T. Kubota, S. Fukutani, T. Ohta and Y. Mahara, J. Radioanal. Nucl. Ch., 2013, **296**, 981-984.
13. L. Szente, É. Fenyvesi and J. Szejtli, Environ. Sci. Technol., 1999, **33**, 4495-4498.
14. A. Bo, S. Sarina, Z. F. Zheng, D. J. Yang, H. W. Liu and H. Y. Zhu, J. Hazard. Mater., 2013, **246**, 199-205.
15. T. Lemesle, F. O. Mear, L. Campayo, O. Pinet, B. Revel and L. Montagne, J. Hazard. Mater., 2014, **264**, 117-126.
16. C. Yan and T. Mu, Phys. Chem. Chem. Phys., 2014, **16**, 5071-5075.
17. X. Zhang, H. Dong, Z. Zhao, S. Zhang and Y. Huang, Energy Environ. Sci., 2012, **5**, 6668-6681.
18. Y. Chen, J. Han, T. Wang and T. Mu, Energy Fuel, 2011, **25**, 5810–5815.
19. K. Ding, Z. Miao, Z. Liu, Z. Zhang, B. Han, G. An, S. Miao and Y. Xie, J. Am. Chem. Soc., 2007, **129**, 6362-6363.
20. Y. Xie, K. Ding, Z. Liu, J. Li, G. An, R. Tao, Z. Sun and Z. Yang, Chem. Eur. J., 2010, **16**, 6687-6692.
21. R. P. Swatloski, S. K. Spear, J. D. Holbrey and R. D. Rogers, J. Am. Chem. Soc., 2002, **124**, 4974-4975.
22. H. Wang, G. Gurau and R. D. Rogers, Chem. Soc. Rev., 2012, **41**, 1519-1537.
23. J. L. Anderson, D. W. Armstrong and G. T. Wei, Anal. Chem., 2006, **78**, 2892-2902.
24. G. Gurau, H. Rodríguez, S. P. Kelley, P. Janiczek, R. S. Kalb and R. D. Rogers, Angew. Chem. Int. Ed., 2011, **50**, 12024-12026.
25. A. Yokozeki, M. B. Shiflett, C. P. Junk, L. M. Grieco and T. Foo, J. Phys. Chem. B, 2008, **112**, 16654-16663.
26. P. Metrangolo, H. Neukirch, T. Pilati and G. Resnati, Accounts. Chem. Res., 2005, **38**, 386-395.
27. A. R. Voth, P. Khuu, K. Oishi and P. S. Ho, Nat. Chem., 2009, **1**, 74-79.
28. C. B. Aakeröy, M. Fasulo, N. Schultheiss, J. Desper and C. Moore, J. Am. Chem. Soc., 2007, **129**, 13772-13773.
29. Y.-Z. Zheng, N.-N. Wang, Y. Zhou and Z. Yu, Phys. Chem. Chem. Phys., 2014, **16**, 6946-6956.
30. J. P. Lommerse, A. J. Stone, R. Taylor and F. H. Allen, J. Am. Chem. Soc., 1996, **118**, 3108-3116.
31. Y.-X. Lu, J.-W. Zou, Y.-H. Wang, Y.-J. Jiang and Q.-S. Yu, J. Phys. Chem. A, 2007, **111**, 10781-10788.
32. H. S. El-Sheshtawy, B. S. Bassil, K. I. Assaf, U. Kortz and W. M. Nau, J. Am. Chem. Soc., 2012, **134**, 19935-19941.
33. H. D. Arman, P. Metrangolo and G. Resnati, Halogen bonding: fundamentals and applications, Springer, 2008.
34. M. G. Sarwar, B. Dragisić, E. Dimitrijević and M. S. Taylor, Chem. Eur. J., 2013, **19**, 2050-2058.
35. C. Walbaum, M. Richter, U. Sachs, I. Pantenburg, S. Riedel, A. V. Mudring and G. Meyer, Angew. Chem. Int. Ed., 2013, **52**, 12732-12735.
36. S. V. Rosokha, C. L. Stern and J. T. Ritzert, Chem. Eur. J., 2013, **19**, 8774-8788.
37. F. Guthrie, J. Chem. Soc., 1863, **16**, 239-244.
38. O. Hassel and K. Stromme, Munksgaard Int Publ Ltd 35 Norre Sogade, Po Box 2148, Dk-1016 Copenhagen, Denmark, 1958, vol. 12, pp. 1146-1147.
39. O. Hassel and K. O. Strømme, Nature, 1958, **182**, 1155 - 1156.
40. W. T. Pennington, T. W. Hanks and H. D. Arman, in Halogen Bonding, Springer, 2008, pp. 65-104.
41. R. S. Mulliken, J. Am. Chem. Soc., 1952, **74**, 811-824.
42. H. A. Benesi and J. Hildebrand, J. Am. Chem. Soc., 1949, **71**, 2703-2707.
43. R. Keefer and L. Andrews, J. Am. Chem. Soc., 1950, **72**, 4677-4681.
44. P. Auffinger, F. A. Hays, E. Westhof and P. S. Ho, Proc. Natl. Acad. Sci. USA, 2004, **101**, 16789-16794.
45. A. Priimagi, G. Cavallo, P. Metrangolo and G. Resnati, Accounts. Chem. Res., 2013, **46**, 2686-2695.
46. P. Metrangolo and G. Resnati, Chem. Eur. J., 2001, **7**, 2511-2519.
47. C. B. Aakeröy, M. Baldrighi, J. Desper, P. Metrangolo and G. Resnati, Chem. Eur. J., 2013, **19**, 16240-16247.
48. A. Bruckmann, M. A. Pena and C. Bolm, Synlett, 2008, 900-902.
49. T. Caronna, R. Liantonio, T. A. Logothetis, P. Metrangolo, T. Pilati and G. Resnati, J. Am. Chem. Soc., 2004, **126**, 4500-4501.
50. P. Metrangolo, T. Pilati, G. Resnati and A. Stevenazzi, Curr. Opin. Colloid In, 2003, **8**, 215-222.
51. Y. Lu, T. Shi, Y. Wang, H. Yang, X. Yan, X. Luo, H. Jiang and W. Zhu, J. Med. Chem., 2009, **52**, 2854-2862.
52. Y. Lu, Y. Wang and W. Zhu, Phys. Chem. Chem. Phys., 2010, **12**, 4543-4551.
53. V. R. Andrea, Curr. Top. Med. Chem., 2007, **7**, 1336-1348.
54. M. Z. Hernandes, S. M. T. Cavalcanti, D. R. M. Moreira, J. de Azevedo, W. Filgueira and A. C. L. Leite, Curr. Drug Targets, 2010, **11**, 303-314.
55. I. Noda, J. Am. Chem. Soc., 1989, **111**, 8116-8118.
56. I. Noda, Appl. Spectrosc., 1990, **44**, 550-561.
57. M. Thomas and H. H. Richardson, Vib. Spectrosc., 2000, **24**, 137-146.
58. S. Morita, H. Shinzawa, I. Noda and Y. Ozaki, Appl. Spectrosc., 2006, **60**, 398-406.
59. M. López-Pastor, M. J. Ayora-Cañada, M. Valcárcel and B. Lendl, J. Phys. Chem. B, 2006, **110**, 10896-10902.
60. Q. Zhang, N. Wang and Z. Yu, J. Phys. Chem. B, 2010, **114**, 4747-4754.
61. N. Wang, Q. Zhang, F. Wu, Q. Li and Z. Yu, J. Phys. Chem. B, 2010, **114**, 8689-8700.
62. L. Zhang, Z. Xu, Y. Wang and H. Li, J. Phys. Chem. B, 2008, **112**, 6411-6419.
63. B. Sun, Q. Jin, L. Tan, P. Wu and F. Yan, J. Phys. Chem. B, 2008, **112**, 14251-14259.
64. B. Sun and P. Wu, J. Phys. Chem. B, 2010, **114**, 9209-9219.
65. Z. Wang and P. Wu, J. Phys. Chem. B, 2011, **115**, 10604-10614.
66. B. Wu, Y. Zhang and H. Wang, J. Phys. Chem. B, 2009, **113**, 12332-12336.
67. Y. Chen, Y. Cao, C. Yan, Y. Zhang and T. Mu, J. Phys. Chem. B, 2014, DOI: 10.1021/jp502995k.
68. Y. Cao, Y. Chen, L. Lu, Z. Xue and T. Mu, Ind. Eng. Chem. Res., 2013, **52**, 2073–2083.
69. Y. Cao, Y. Chen, X. Sun, Z. Zhang and T. Mu, Phys. Chem. Chem. Phys., 2012, **14**, 12252-12262.
70. Y. Cao, Y. Chen, X. Sun and T. Mu, CLEAN–Soil, Air, Water, 2013, **41**, 1-8.

This journal is © The Royal Society of Chemistry [year]